

## THE TRANSIENT STRESS FIELD NEAR THE TIP OF A STATIONARY CRACK IN A MATERIAL UNDERGOING CREEP-CONSTRAINT GRAIN BOUNDARY CAVITATION

V. BANTHIA and C. Y. HUI

Department of Theoretical and Applied Mechanics, Cornell University, Ithaca,  
NY 14853, U.S.A.

(Received 8 October 1986; in revised form 10 August 1987)

**Abstract**—The influence of cavitation on the transient stress field near the tip of a Mode I plane strain stationary crack is examined using a phenomenological constitutive model proposed by Hutchinson for the steady state creep of polycrystalline materials under creep constrained grain cavitation. The time history of the amplitude of the singular stress field near the crack tip is computed for the special case of a plane strain edge crack under a suddenly applied constant load. The effect of non-uniform distribution of cavitating facets on the near tip stress field is analyzed by assuming that the density of a cavitating facet is piecewise constant.

### INTRODUCTION

At an elevated temperature crack growth in a polycrystalline metal often occurs by the growth and coalescence of grain boundary voids. Void growth can occur by means of the following mechanisms: (1) the diffusive transport of atoms along the grain boundary[1], (2) the creep deformation of the grains by power law creep[2], (3) coupled diffusion and power law creep[3]. In general, void growth is determined by the coupling of the mechanism of coupled diffusion and power law creep. However, under the conditions of sufficiently low stresses, power law creep becomes less important as far as the kinetics of void growth is concerned, i.e. locally a void grows by the process of diffusion. The local dominance of the diffusive mechanism, however, does not necessarily imply that the actual void growth rate can be calculated on the basis of diffusion alone. As Dyson first pointed out[4], growth of voids on relatively isolated grain boundary facets under the condition of low applied stresses is necessarily dependent on the surrounding grains which have to deform continuously by creep to accommodate the matter diffusing away from the growing voids. Thus, the stress, on a grain boundary facet, which equals the applied macroscopic stress at the instant of loading (assuming the instantaneous response of the material is elastic) will relax with time. This means that the stress acting on the cavitating grain boundary may be very different from the macroscopically applied stress. Rice[5] quantified Dyson's concept by showing that, in a material where cavitated grain boundaries are relatively isolated from each other, the overall void growth rate is determined in the low stress limit by power law creep. Riedel[6] generalized the result of Rice to multiaxial states of stress. Riedel also computed the time  $t_r$  for the stress carried by the cavitating facets to be completely relaxed. For time larger than  $t_r$ , cavitating grain facets can be considered to behave effectively as traction-free microcracks.

Based on Dyson's concept described above, Hutchinson proposed a phenomenological constitutive model for the steady creep of polycrystalline material undergoing creep constrained grain boundary cavitation[7]. The grain boundary facets in this model are assumed to be traction-free penny-shaped cracks and are embedded in a power law creeping material. It is assumed that only facets which are aligned normal to the maximum principal tensile stress direction can cavitate and that the spacing between the cavitating facets is sufficiently large so that their interaction can be neglected. With these assumptions, Hutchinson derived the potential function for this material. He also showed that the stress singularity ahead of a stationary crack tip in the material is still given by that of the HRR field. By assuming that the density of the cavitating facets is uniform near the crack tip and that transient or

elastic deformation can be ignored, Hutchinson showed that the strength of the HRR singularity is determined by the well-known path integral  $C$  [7].

Tvergaard [8, 9] has extended Hutchinson's constitutive model to account for non-zero traction on the micro-crack faces and for the grain boundary sliding. He also completed a numerical study of creep crack growth based on his model [10]. In this work, we will focus on Hutchinson's model and its effect on the transient near tip stress distribution of a stationary crack.

The influence of cavitation on the transient stress fields near the tip of a stationary crack is studied by including the instantaneous elastic deformation in Hutchinson's constitutive model. Thus, at the instant of loading, the crack tip field is governed by the elastic  $K$  field. For sufficiently short times, the creep zone is small compared with the region of validity of the  $K$  field, the small scale creep (S.S.C.) problem is therefore well posed. The transient stress field near the crack tip under S.S.C. conditions will still be governed by  $K$ . We will begin this work by analyzing this S.S.C. problem. For short times, an approximate formula can be obtained for the transient stress near the crack tip. Assuming that the loading remains constant, the S.S.C. condition will eventually be violated and extensive creep occurs everywhere. The time of transition from S.S.C. to extensive creep is estimated. The transition from S.S.C. to steady state is also examined by means of a finite element study of an edge crack under plane strain and constant Mode I loading conditions. The finite element calculations are performed assuming that  $\rho$ , a parameter which measures the density of cavitating facets, is spatially uniform. Comparisons are made with the short-time solution, the approximation for the transient amplitude of the singular field and the estimated transition time for different values of  $\rho$ .

In general, the density of the cavitating facets is not spatially uniform and is most probably a decreasing function of the distance away from the crack tip. Under this condition, the proof of the path independence of the  $C$  integral breaks down even if the "steady state" condition of extensive creep occurs everywhere. It may, however, still be possible that the "far field" value of the line integral may not be too different from its near tip value. This question is investigated in this work by repeating our finite element calculations with a piecewise constant  $\rho$ . Specifically, we assume that  $\rho = \text{constant}$  in a circular region engulfing the crack tip and that  $\rho = 0$  outside this circle. The radius  $d$  of this circular region is assumed to be of order  $r_K$ , where  $r_K$  denotes the extent of the region of asymptotic validity of the elastic  $K$  field if the specimen is linearly elastic. It is probably unlikely that this distribution of cavitating facets occurs, our choice is based on the following rationale.

(1) The distribution of the cavitating facets cannot be known in advance and is inherently an unknown of the problem. We therefore pick a distribution that is simple to implement in the numerical scheme.

(2) It is easy to interpret the results since the  $C$  integral is path independent both outside and inside the circle. The question reduces, therefore, to the magnitude of the jump of the value of this integral across the boundary of the circle.

#### FORMULATION OF GOVERNING EQUATIONS

A small strain and displacement theory is used in which the strain displacement equations and the equilibrium equations are linear. We use a coordinate system  $(x, y, z)$  with the  $z$ -axis lying along the crack front together with a cylindrical coordinate system  $(r, \theta, z)$ . The origins of both coordinate systems are attached to the crack tip. In this work attention is directed to the case of plane strain Mode I loading.

We assume that the total strain rate tensor  $\dot{\epsilon}$  consists of two parts, i.e.

$$\dot{\epsilon}_{ij} = \dot{\epsilon}_{ij}^e + \dot{\epsilon}_{ij}^c \quad (1)$$

where  $\dot{\epsilon}_{ij}^e$  and  $\dot{\epsilon}_{ij}^c$  denote the Cartesian components of the elastic and creep strain rate tensor, respectively. The elastic strain rate is related to the stress rate through the isotropic Hooke's law. In Cartesian coordinates, they are

$$\dot{\epsilon}_{ij}^c = (1 + \nu)\dot{\sigma}_{ij}/E - \nu\dot{\sigma}_{kk}\delta_{ij}/E \quad (2)$$

where  $\nu$  is Poisson's ratio and  $E$  is Young's modulus. The creep strain rate is related to the stresses by [7]

$$\dot{\epsilon}_{ij}^c = (3/2)B\sigma_e^n \{s_{ij}/\sigma_e + \rho[\mu_n(s_{ij}/\sigma_e)(S/\sigma_e)^2 + 2Sm_{ij}/(n+1)\sigma_e]\} \quad (3)$$

where  $s_{ij}$  is the component of the stress deviator in Cartesian coordinates,  $S$  the maximum principal stress,  $\sigma_e$  the equivalent stress and  $\mu_n \equiv 3(n-1)/2(n+1)$ .  $\mathbf{m}$  is the tensor the components of which in the principal axes of stress are

$$m_{ij} = \delta_{iK}\delta_{jK} \quad (\text{no sum on } K) \quad (4)$$

where  $\delta_{ij}$  is the Kronecker delta and  $K$  denotes the index associated with the direction aligned with the maximum principal tensile stress  $S$ . The factor  $\rho$  in eqn (3) is related to the density of the cavitating facets  $N$  by

$$\rho = 4b^3 N(n+1)(1+3/n)^{-1/2} \quad (5)$$

where  $b$  is the radius of the cavitating facets. We shall assume  $\rho$  to be a function of position only. When  $\rho = 0$ , eqn (3) reduces to the well-known power law creep model with  $n$  being the creep exponent and  $B$  a temperature-dependent material parameter. Note that the existence of cavitating facets contributes an additional distortional component to the creep strain rate. In particular, for non-vanishing  $\rho$ , the dilational creep strain rate is generally nonzero.

The material description, eqns (1)–(3), is supplemented by the equilibrium equations which are linear and is satisfied identically by the introduction of the Airy stress function  $\phi$ , i.e.

$$\sigma_{ij} = -\phi_{,ij} + \phi_{,kk}\delta_{ij} \quad (6)$$

with respect to the Cartesian coordinate system  $(x, y)$ . The governing partial differential equation can then be derived by inserting eqn (6) into eqns (1)–(3) and then inserting the resulting strain rate tensor into the compatibility equation for plane strain.

#### ASYMPTOTIC STRESS FIELD

The transient asymptotic stress field near the tip of a stationary crack follows quite easily from the analysis of Riedel and Rice [11]. From asymptotic dominance, it can be shown that for  $n > 1$ , the elastic terms in the governing equations can be neglected if the crack is stationary and the stress field near the crack tip is given by HRR field, i.e.

$$\sigma_{ij} = (A(t)/BIt)^{1/(n+1)}\bar{\sigma}_{ij}(\theta, \rho) \quad (7)$$

where  $\bar{\sigma}_{ij}(\theta, \rho)$  are dimensionless functions describing the angular variation of the near tip stress field. The numerical analysis of Hutchinson [7] showed that these functions are weakly dependent on  $\rho$ .  $I = I(n, \rho)$  is a numerical constant dependent on  $n$  and  $\rho$ . The numerical results of Ref. [7] showed that  $I(n, \rho)$  is related to  $I = I(n, 0)$  approximately by

$$I(n, \rho) = I_0(n) + \rho I_1(n). \quad (8)$$

Values of  $I_0$ ,  $I_1$  for different values of  $n$  can be found in Ref. [7]. We note that the existence of the asymptotic field (7) does not depend on the assumption that  $\rho$  is uniform. Indeed, eqn (7) is valid as long as  $\rho$  is bounded at  $r = 0$ . If  $\rho$  is nonuniform, then  $\rho$  in eqn (7) must be interpreted as the value of  $\rho$  at the crack tip. From eqn (3), the creep strain and the strain rate must necessarily have an  $r^{-n/(n+1)}$  singularity at  $r = 0$ . The time-dependent amplitude  $A(t)$

cannot be determined by asymptotic analysis and is dependent on the loading history. Under conditions for which there exists a unique stress-strain rate relation (e.g. extensive creep conditions where the elastic strain rate is insignificant compared to the steady state creep rate given by eqn (3) everywhere),  $A(t)$  is dependent on the external loading, the geometry of the body and  $n$ . Furthermore, if  $\rho$  is constant in a region  $\Omega$  enclosing the crack tip,  $A(t)$  is given by the path integral  $C$  which is independent of path for all contours  $\Gamma$  in  $\Omega$  encircling the crack tip. In general, the  $C$  integral is path dependent and is defined by

$$C(t) = \int_{\Gamma} \{ [n/(n+1)] \sigma_{ij} \dot{\epsilon}_{ij} n_i - \sigma_{ij} n_j \dot{u}_{i,1} \} ds. \quad (9)$$

In eqn (9),  $\mathbf{n}$  denotes the outward normal to  $\Gamma$ ,  $\dot{u}_i \equiv u_{i,t}$  is the displacement rate at a material point. In regions where the creep strains are much greater than the elastic strains,  $\sigma_{ij} \dot{\epsilon}_{ij} = B \sigma_e^{n+1} (1 + \rho(S/\sigma_e)^2)$ . Note that the conditions: (1) existence of unique stress-strain rate relation, (2)  $\rho = \text{constant}$  (material homogeneous) both must be satisfied for the  $C$  integral to be path independent. The second condition can be relaxed if the material is homogeneous in the  $x$ -direction (i.e.  $\rho = \rho(y)$ ). It is, however, unlikely that  $\rho = \rho(y)$  in metals except under very special circumstances (e.g. composite materials).

#### SMALL SCALE CREEPING

The presence of the elastic term in eqn (1) allows for the instantaneous response of the material subjected to a sudden applied load. As the accumulation of creep strain cannot be instantaneous, at the instant of loading, the stress field in the material body must be determined by the elastic term in eqn (1) alone. The crack tip field at  $t = 0$  must therefore be the elastic  $K$  field. For sufficiently small times, with the exception of a region the size of which is very small compared with the region of dominance of the  $K$  field, the accumulated creep strain is small compared with the elastic strain and the near tip deformation field must necessarily still be governed by  $K_I$ . This will be referred to as the small scale creeping (S.S.C.) condition. In the S.S.C. problem, the region of dominance of the  $K$  field is mathematically taken as infinite as it is large compared with the creep zone, which will be defined as the boundary where the equivalent elastic strain and the equivalent creep strain are equal. Within the creep zone one expects the stresses to relax with time (except for  $n = 1$ ). Assuming that the external loading does not decrease with time the creep zone will grow sufficiently large as time increases so that the S.S.C. condition can no longer be satisfied in a finite specimen. Thus, the solution to the S.S.C. problem is asymptotic and is a short-time solution.

We will now consider the S.S.C. problem of a material obeying a constitutive model of the form of eqns (1)–(3) under a suddenly applied load which is held constant thereafter. We will also assume that  $\rho$  is constant everywhere in the S.S.C. problem. That is,  $\rho$  is constant inside the region of dominance of the  $K$  field. In a specimen the size of which is large compared with the crack length  $a$ , the region of  $K$  dominance is of the order of  $0.1a$ . The initial condition for the S.S.C. problem is

$$\sigma_{ij}(r, 0) = K_I f_{ij}(\theta) / (2\pi r)^{1/2} \quad (10)$$

as  $t \rightarrow 0$ . The  $f_{ij}$ 's are universal functions describing the angular variation of the stresses. The boundary conditions are the usual traction free boundary conditions on the crack faces. Following Riedel and Rice[11], the stress for this problem must have the self-similar form

$$\sigma_{ij} = (EBt)^{-1/(n+1)} F_{ij}(R, \theta, n, \nu, \rho) \quad (11a)$$

where  $R$  is a dimensionless radial distance given by

$$R = (EBt)^{-2(n-1)}r/K_1^2. \quad (11b)$$

For  $t > 0$  and  $r \rightarrow 0$ , the stress near the crack tip is given by eqn (7) and is the HRR field. Therefore,  $F$  must behave as [11]

$$F_{ij}(R, \theta, n, \nu, \rho) = \beta_n R^{-1(n+1)} \bar{\sigma}_{ij}(\theta) \quad (12)$$

when  $R \rightarrow 0$ , where  $\beta_n$  is a numerical constant dependent on  $n$ ,  $\rho$  and  $\nu$ . The amplitude  $A(t)$  of the near tip stress field is given by combining eqns (7) and (12)

$$A(t) = I\beta_n^{n+1} K_1^2 / Et. \quad (13)$$

Equation (13) implies that, within the region of asymptotic validity of these fields, the stresses relax as  $t^{-1(n+1)}$ . Since  $\epsilon_{ij}^e / \dot{\epsilon}_{ij}^e \rightarrow 0$  (no sum on  $i$  and  $j$ ) as  $r \rightarrow 0$ , the asymptotic strain rate field at the crack tip is given by

$$\dot{\epsilon}_{ij} \sim \dot{\epsilon}_{ij}^e \quad (14a)$$

where the asymptotic stress field, eqns (7) and (3), must be used to evaluate  $\dot{\epsilon}_{ij}^e$ . From eqns (14a) and (7), the asymptotic strain field is

$$\epsilon_{ij} \sim \epsilon_{ij}^e = (n+1)t\dot{\epsilon}_{ij}^e. \quad (14b)$$

Equations (14a) and (14b) are approximately valid as long as  $r$  is in the region of asymptotic validity of the HRR field. Equations (7) and (14a) point out that there is a total relationship between the stress and strain rate field. An equivalent way of saying this is that the material near the crack tip can be replaced by a cavitated material undergoing steady state creep. This, together with our assumption of  $\rho = \text{constant}$ , implies that the  $C$  integral is path independent near the crack tip for each instant in time and that  $A(t)$  must be approximately equal to  $C(t)$  evaluated in this region. Note that

$$A(t) = C(t) \quad (15)$$

at the crack tip as long as  $\rho$  is bounded at the crack tip.

As in Riedel and Rice [11], the creep zone boundary  $R_c(t)$  can be estimated by calculating the equivalent strains  $\epsilon_c^e$  and  $\dot{\epsilon}_c^e$  using the asymptotic stress fields, eqns (10) and (7), and then setting them equal to each other. The result is

$$R_c(t, \theta) = K_1^2 [EBt]^{2(n-1)} F_c(\theta, \rho, n, \nu) \quad (16)$$

where  $F_c$  is a dimensionless function describing the angular variation of the creep zone boundary and is dependent on  $n$ ,  $\rho$  and  $\nu$ . The creep zone size increases with time proportional to  $t^{2(n-1)}$  under S.S.C.

The exact value of  $\beta_n$  or  $C(t)$  can only be determined by the complete solution of the S.S.C. problem or by finding the short time near the tip stress field of any plane strain specimen under Mode I loading under S.S.C. conditions. The solution of the latter problem will be presented in the next section. We now use a method used by Riedel and Rice [11] to estimate  $\beta_n$ . Riedel and Rice proposed to estimate  $\beta_n$  by assuming that the  $J$  integral is approximately path independent everywhere. This assumption may be justified by the following observations. (1)  $J$  is approximately path independent inside the region of asymptotic validity of the HRR field, since in this region there is an approximate total relation between strain and stress; (2)  $J$  is path independent at distances large compared with the creep zone since the material there is linearly elastic (S.S.C.).

Near the crack tip  $C(t)$  can be obtained by using the relation  $C = J/(n+1)t$  in the crack tip region which can be derived using eqns (7), (14) and the definition of  $J$  and  $C$ . At the crack tip, therefore

$$A(t) = C(t) = J_{\text{tip}}/(n+1)t \quad (17)$$

where  $J_{\text{tip}}$  is the value of the  $J$  integral evaluated at  $r = 0$ . The assumption of path independence of  $J$  implies that

$$J_{\text{tip}} = J(r \rightarrow \infty) = (1 - \nu^2)K_I^2/E. \quad (18)$$

Using eqn (13),  $\beta_n$  is estimated to be

$$\beta_n \sim [(1 - \nu^2)/(n+1)I]^{1/(n+1)}. \quad (19)$$

Equation (19) reduces to the result of Riedel and Rice in the special case of  $\rho = 0$ . It should be noted that  $\beta_n$  in this work is related to  $\alpha_n$  in the work of Riedel and Rice by the relation  $\beta_n = \alpha_n[n/(n+1)^2\pi]^{1/(n+1)}$ . For the special case of  $\rho = 0$ , Ehlers and Riedel[15] have shown that  $\beta_n$  given by eqn (19) differs from their numerical results by no more than 4%.

The characteristic time  $t_T$  for the transition from S.S.C. to extensive creep of the whole specimen can be estimated if one further assumes that  $\rho = \text{constant}$  in the whole specimen and not just in the region of validity of the  $K$  field. In this case the final steady state value of  $C(t) = C^*$  integral is path independent. Following Riedel and Rice[11],  $t_T$  is estimated by equating the short-time limit of  $C(t)$  given by eqn (13) and the long time steady state limit,  $t_T$  is found to be

$$t_T = I\beta_n^{n+1}K_I^2/(EC^*) \quad (20)$$

which is identical to the result of Riedel and Rice with  $I_n$  in their work replaced by  $I$ .

#### NUMERICAL RESULTS FOR THE CASE $\rho = \text{CONSTANT}$

The finite element method is used to obtain the time-dependent stress field of a plane strain edge crack of length  $a$  under tensile loading conditions. The edge crack configuration is shown in Fig. 1. To simulate an edge crack of length  $a$  in an elastic half space, the square boundary where loading is applied is taken to be of  $31a$  and is centered at the crack tip at the origin. Initially, the stress and strain field of the body is taken to be zero. At time  $t = 0$ , a tensile load of  $\sigma_{xx} = \sigma_n$  is applied to the remote boundary and thereafter held constant. Traction free boundary conditions are prescribed on the crack faces  $-a < x < 0$ ,  $y = 0$  and the surface  $x = -a$ . As the crack is loaded in Mode I we need only to consider the domain  $y > 0$ , with boundary conditions on the positive  $x$ -axis given by  $u_{yy} = \sigma_{xy} = 0$ . The configuration and loading conditions we adopted in this work are similar to the work of Bassani and McClintock[12], who considered the special case of  $\rho = 0$  (an elastic power law creeping material). The results of the finite element analysis are presented in this section. Details of our numerical procedure are given in the Appendix.

The time scale used in this numerical study is obtained by finding the time  $t_\rho$  for the creep strain to equal the elastic strain under a uniaxial tensile stress  $\sigma_n$ .  $t_\rho$  is found to be

$$t_\rho = (\sigma_n/E)/\{(1+\rho)\dot{\epsilon}_n^c(\rho=0)\} \equiv t_0/(1+\rho) \quad (21)$$

where  $\dot{\epsilon}_n^c(\rho=0) \equiv B\sigma_n^n$ . Since  $t_0 \equiv \sigma_n/E\dot{\epsilon}_n^c(\rho=0)$  is independent of  $\rho$ ,  $t_\rho$  is a monotonic decreasing function of  $\rho$ .

At time  $t = 0$  the response of the material is elastic. The stress intensity factor evaluated at time  $t = 0$  by our finite element calculation is accurate to within 1% of the exact analytical result of  $K_I = 1.12\sigma_n(\pi a)^{1/2}$ . To assess the accuracy of our program, we considered the special case of  $\rho = 0$  (no cavitation) first. The numerical result for the case of  $n = 3$  and  $\rho = 0$ , was obtained by Bassani and McClintock[12]. Graphed in the same scale as their publication, the difference between our numerical results and theirs is less than a pen width. A further check on our numerical scheme is to compare the steady state value of  $C = C^*$  with the bounds established by He and Hutchinson[13]. They have established very accurate

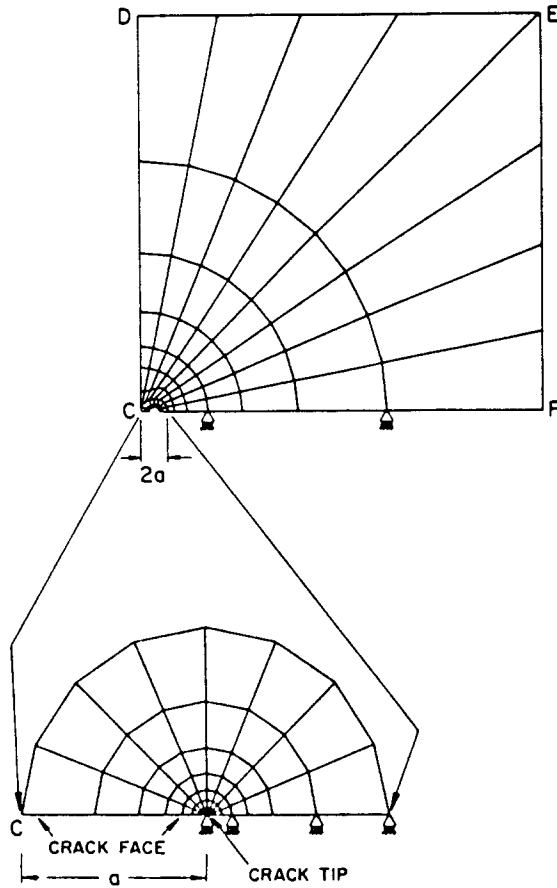


Fig. 1. Finite element mesh used to compute the time-dependent deformation field of a plane strain edge crack of length  $a$  loaded in Mode I. The sides CD, DE, EF and FC are of equal length  $L = 31a$ . A magnified view of the mesh in the crack tip region is also shown in the figure.

upper and lower bounds for  $J$  for the case of a plane strain Mode I edge crack in a power law hardening material. Their  $J$  values can be easily converted to  $C^*$  for a power law creeping material ( $\rho = 0$ ). For  $n = 3$ , the upper and lower bounds for  $C^*$  are 3.54 and 3.70, respectively[13], whereas our numerical result gives  $C^* = 3.95$ . For the case of  $n = 5$ , a very large number of time steps are required for  $C(t)$  to converge to the steady state value of  $C^*$ . The steady state value of  $C(t)$  is not shown in Fig. 3.

Figures 2 and 3 show the normalized time history of the normalized  $C(t)$  for the case of  $n = 3$  and 5, respectively. The values of  $\rho = 0, 0.5$  and 1.0 were used for each value of  $n$ . The details of the evaluation of  $C(t)$  are given in the Appendix. The values of  $C(t)$  presented below are the ones calculated over the circular path nearest to the crack tip ( $r = 0.002a$ ). At very short time, before the creep zone has had time to grow appreciably, the value of  $C(t)$  calculated over different paths in our mesh differs considerably. However, as the creep zone grows, more and more of the paths close to the crack tip lie completely within the creep zone and  $C(t)$  evaluated over these paths becomes path independent.

Figures 2 and 3 show that, with respect to the normalized time

$$T \equiv t/t_\rho$$

the normalized values of  $C(T, \rho)$  for different values of  $\rho$  collapse into one single curve. Thus, our numerical results show that

$$C(T, \rho)/I \sim C(T, 0)/I_0. \tag{22}$$

Since the amplitude of the near tip stress field depends on  $C/I$  ( $B$  is independent of  $\rho$ ), eqn

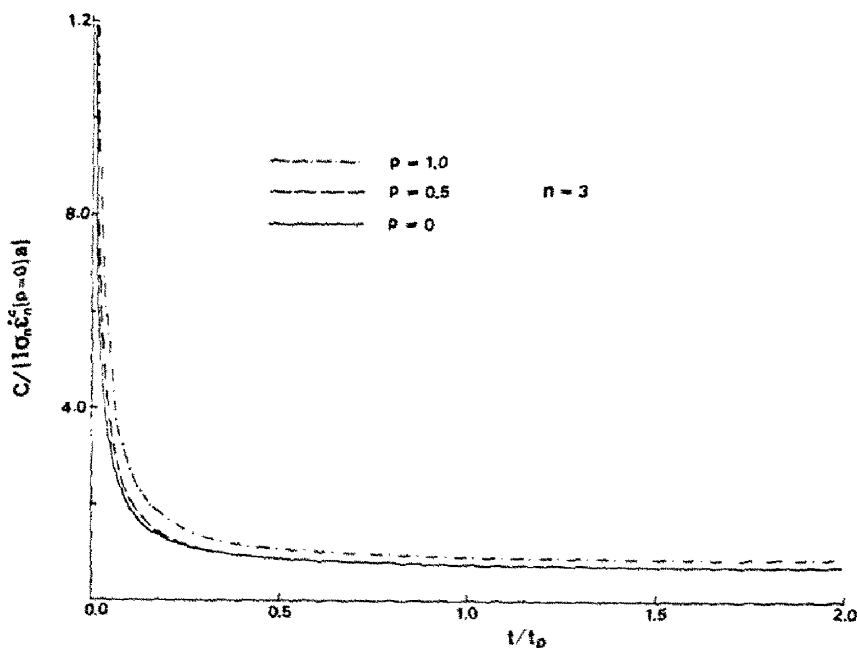


Fig. 2. Normalized time history of normalized  $C(t, \rho)$  for the case of  $n = 3$  with  $\rho = 0, 0.5$  and  $1.0$ , respectively.

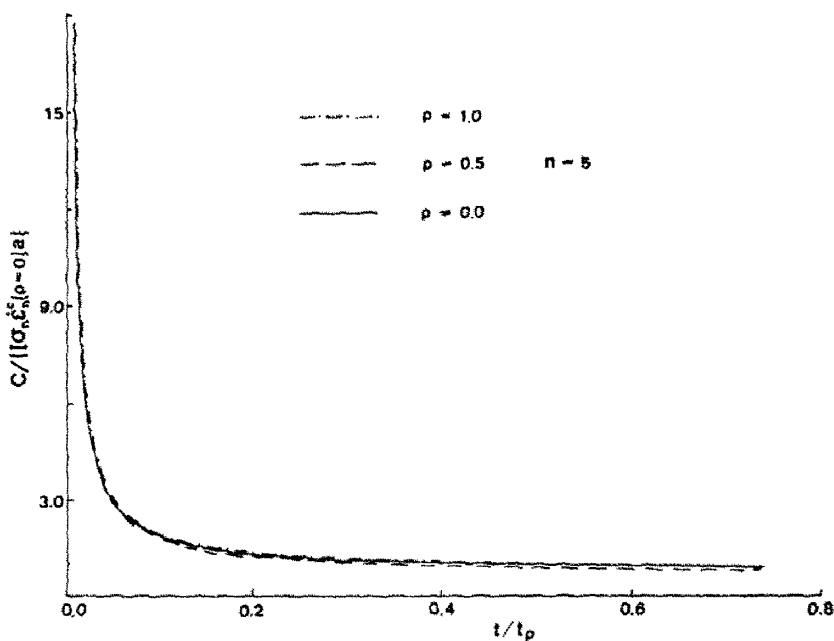


Fig. 3. Normalized time history of normalized  $C(t, \rho)$  for the case of  $n = 5$  with  $\rho = 0, 0.5$  and  $1.0$ , respectively.

(22) and Figs 2 and 3 imply that the near tip stresses are monotonic decreasing functions of  $\rho$  for each fixed  $r$  and  $t$ . This is expected as the cavitation increase the amount of creep straining and hence stress relaxation increases as  $\rho$  increases. A consequence of this numerical result is that for non-zero  $\rho$  the transition time  $t_T$  from S.S.C. to extensive creep is given by

$$T_T(\rho) = t_T(\rho = 0)/(1 + \rho) \tag{23}$$

by eqn (21). Equation (22) shows that the steady state value of  $C^*$  is given approximately by



$$C^*(\rho) \sim (I(n, \rho)/I_0)C^*(\rho = 0). \quad (24)$$

Therefore, the steady state value of  $C \equiv C^*$  is a monotonic increasing function of  $\rho$  for fixed values of  $n$ . Since the strengths of the near tip stresses under steady state creeping conditions depends only on  $C^*/I$ , eqn (24) implies that for a plane strain edge crack in an infinitely extended body undergoing extensive creep, the strength of the near tip fields are independent of  $\rho$  as long as  $\rho$  is spatially uniform.

Since the normalized  $C$  vs  $T$  curves are independent of  $\rho$ ,  $\beta_n(\rho)$  can be related to  $\beta_n(\rho = 0)$  by eqns (13) and (15).  $\beta_n$  is found to be

$$\beta_n(\rho) = [1 + \rho]^{-1/(n+1)}\beta_n(\rho = 0). \quad (25)$$

Equation (25), which is a consequence of our numerical work, differs from  $\beta_n$  obtained from assuming the path independence of  $J$  by a numerical factor of  $[(1 + \rho)I_0/I]^{1/(n+1)}$ . It provides a good approximation to  $\beta_n$  as  $\beta_n(\rho = 0)$  agrees with numerical results to within 4%.

Using  $\beta_n$  and  $C^*$  given by eqns (25) and (24), respectively, we found, as expected, there is an exact agreement between the  $t_T$  given by eqns (23) and (20).

Equations (13) and (15) predict that, for short times,  $C$  is inversely proportional to time  $t$ . We have found that, log-log plots of  $C(t)$  vs normalized time curves have slopes ranging from  $-0.9$  to  $-1.1$  for times less than  $t_T$  for all cases.

Time sequences of the creep zone boundaries for  $\rho = 0, 0.5$  and  $1.0$  are obtained from our numerical results for the cases of  $n = 3$  and  $5$ , respectively. For short times ( $t/t_T < 1$ ), these zones propagate roughly with a self-similar shape. As expected, the extent of the creep zone is a monotonic increasing function of  $\rho$  at any fixed instant in time. For  $t/t_T > 1$ , the creep zones approach the boundary and lose their self-similar shape.

#### NUMERICAL RESULTS FOR A PIECEWISE CONSTANT $\rho$

We considered the same problem as in the previous section except that  $\rho$  is now taken to be piecewise constant. Specifically, we assume that  $\rho = \rho_{up} = \text{constant}$  in a circular region engulfing the crack tip and that  $\rho = 0$  outside this circle. The radius  $d$  of this circular region is assumed to be of order  $r_K$ , where  $r_K$  denotes the extent of the region of asymptotic validity of the elastic  $K$  field if the specimen is linearly elastic. In the following calculations  $r_K$  is taken to be  $0.1a$ . With this choice of  $d$ ,  $\rho$  can be considered to be spatially uniform as far as the S.S.C. problem is concerned. Indeed,  $\rho$  can be considered to be spatially uniform for the S.S.C. problem as long as  $d > r_K$ . We therefore expect the deformation fields for the case of piecewise constant  $\rho$  to be approximately the same as that of the case of  $\rho = \rho_{up}$  everywhere as long as the S.S.C. condition prevails. For time larger than  $t_T$ , S.S.C. no longer exists and the stresses would be different from that of the case where  $\rho$  is spatially uniform. The case of  $n = 3$  is used in the numerical study below. Values of  $\rho$  used in this study are taken to be  $\rho = 0.5$  and  $1.0$  for  $r < d$  and  $\rho = 0$  for  $r > d$ , respectively.

Of particular interest is whether the steady state value of the  $C(t)$  integral,  $C^*$ , is approximately path dependent. Our choice of  $\rho$  implies that  $C^*$  is path independent in the region inside and outside of the circle. The discontinuity of  $\rho$  causes some components of the stress and strain tensor to be discontinuous across the circular boundary. We therefore anticipated that  $C^*$  is discontinuous across the boundary of the circle.

The time evolution of the normalized  $C(T)$  was studied for the two cases stated above. As anticipated, for time smaller than the transition time given by eqn (20), the time history of  $C/I$  for paths inside the creep zone for the case of piecewise constant  $\rho$  are practically identical to the case of uniform  $\rho$  discussed in the previous section. For times larger than the transition time  $t_T$ ,  $C(t, \rho)/I \sim C^*/I$  for the two cases are different. The  $C^*/I$  associated with the piecewise constant  $\rho$  is lower in value than the spatially uniform case of  $\rho = 1$  in the region  $r < d = 0.1a$ . The normalized  $C^*$  as a function of normalized radial distance  $r/a$

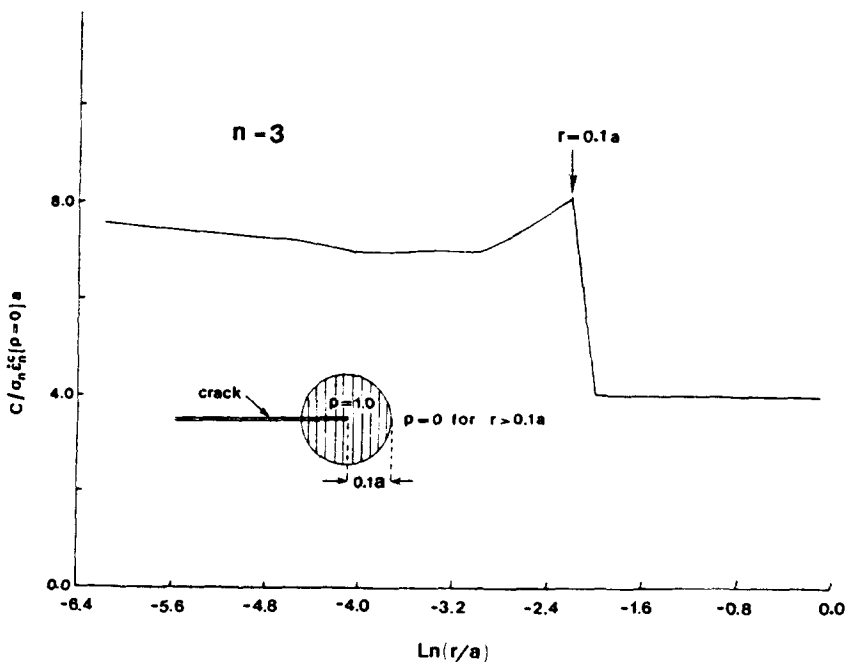


Fig. 4. Normalized steady state value of  $C(t, \rho) = C^*$  as a function of normalized distance  $r/a$  from the crack tip for the case of  $n = 3$ ,  $\rho = 0$  and 1.0, respectively.

is shown in Fig. 4. The  $C^*$  integrals evaluated on different paths inside the region  $r < 0.1a$  differ from each other by less than 4%. The average normalized value of  $C^*$  in this region is 7.0 as compared to 16.7 for the spatial uniform case of  $\rho = 1$ .

As expected, the numerical results show that these long time  $C^*$  integrals are path independent both inside and outside of the circle  $r = 0.1a$ . Figure 4 shows that, in the region  $\rho = 0$ , the steady state value of normalized  $C^*$  is practically the same as the case of a spatially uniform  $\rho$  (4.02 vs 3.98). However, the difference between the normalized values of  $C^*$  inside and outside  $r = 0.1a$  is significant. The normalized value of  $C^*$  outside the circle is 4.02 which is almost 50% less than the inner  $C^*$  value of 7.0.

#### SUMMARY AND DISCUSSION

Our numerical results show that results for the case  $\rho = 0$  can be easily generalized to that of  $\rho \neq 0$  if we assumed that  $\rho$  is spatially constant. Note that, although  $\rho$ , the density of cavitating facets is spatially uniform, the rate of cavitation and growth of voids is a strong function of position. As in the case of  $\rho = 0$ , the S.S.C. condition can be characterized by the condition  $t_T(\rho) < 1$ . Under S.S.C., the near tip deformation field is controlled by the elastic stress intensity  $K_I$ . The amplitude of the HRR field under S.S.C. under a suddenly applied constant load is determined by the numerical constant  $\beta_n(\rho)$  in eqn (13). Our finite element analysis indicates that  $\beta_n(\rho)$  is related to  $\beta_n(\rho = 0)$  by the simple expression (25). Furthermore, the transition time  $t_T$  for non-zero  $\rho$  is lower than  $t_T(\rho = 0)$  by a factor of  $1/(1 + \rho)$ . The ratio of the steady value of  $C(t \rightarrow \infty) = C^*$  for non-zero  $\rho$  to  $C^*(\rho = 0)$  is found numerically to be approximately given by  $I/I_0$  for each fixed  $n$ . A consequence of this result is that the near tip steady state deformation fields for the case of the edge crack geometry we considered are independent of  $\rho$  as long as  $\rho$  is spatially uniform. It is not clear if this particular result is independent of specimen geometry. Further numerical studies are needed to clarify this point. If this result were independent of specimen geometry, it would imply that for a specimen undergoing extensive creep, the deformation fields near the crack tip depends only on  $C^*/I$  and are otherwise independent of  $\rho$ .

We have also carried out a numerical study of a case where  $\rho$  is not spatially uniform and is piecewise constant. Our results show that, as long as the region of non-zero (but constant)  $\rho$  is sufficiently large so that it engulfs the region of asymptotic validity of the  $K$

field at  $t = 0$ , the distribution of the deformation field does not differ significantly from the case of uniform  $\rho$  everywhere in the specimen. This result is consistent with the S.S.C. assumption. However, we do find that there is a significant difference between the steady value of  $C \equiv C^*$  inside the circular region where  $\rho = \text{constant} \neq 0$  and outside the region where  $\rho = 0$ . However, the case of piecewise constant  $\rho$  is probably the case where the discrepancy between the "inner"  $C^*$  value of the "outer"  $C^*$  value is the largest. It could still be possible, in situations where  $\rho$  varies continuously with distances away from the crack tip, that the  $C^*$  integral is approximately path independent.

There are obvious limitations associated with the constitutive model used in this study. Hutchinson's phenomenological model is derived based on a dilute concentration of cavitated grain facets so that interaction between the cavitated facets can be ignored. This is highly unlikely near the crack tip region where stresses are high. Furthermore, it is not clear how  $\rho$  should be determined in the crack tip region. In general, one would expect  $\rho$  to evolve as a function of stress in the crack tip region. Equations governing the evolution of  $\rho$  are as yet unavailable. The steady state creep law stated by eqn (3) was derived on the basis that the stress carried by the cavitating facets is completely relaxed. Therefore, our calculation is valid only when  $t_{\text{f}}$  is sufficiently larger than  $t_{\text{r}}$ . Also, our analysis ignores the effect of geometry changes (small strain theory and a mathematically sharp crack is assumed in our calculations) and hence cannot be uniformly valid in the crack tip region. The region near the crack tip where finite strain effects are important is about one or two crack opening displacements. Our analysis is expected to be valid outside this region.

*Acknowledgement*—C. Y. Hui was supported by the NSF grant NSF 84-00776. Vinod Banthia was supported by the NSF grant CEE 8206344. C. Y. Hui would like to thank K. C. Wu for discussions and editorial comments.

#### REFERENCES

1. T. J. Chuang, K. I. Kagawa, J. R. Rice and L. Sills, Non-equilibrium models for diffusive cavitation of grain interfaces. *Acta Metall.* **27**, 265 (1979).
2. A. Needleman and J. R. Rice, Plastic flow effects in diffusive cavitation of grain boundaries. *Acta Metall.* **28**, 1315 (1980).
3. B. Budiansky, J. W. Hutchinson and S. Slutsky, Void growth in viscous solids. In *Mechanics of Solids*, The Podney Hill 60th Anniversary Volume (Edited by H. G. Hopkins and M. J. Sewell), p. 13. Pergamon Press, Oxford (1982).
4. B. F. Dyson, Constraints on diffusional cavity growth rates. *Metal Sci.* **10**, 349 (1976).
5. J. R. Rice, Constraints on the diffusive cavitation of isolated grain boundary facets in creeping polycrystals. *Acta Metall.* **29**, 675 (1981).
6. H. Riedel, Constraint grain boundary cavitation in a creeping body containing a macroscopic crack. *Fourth International Conference on Mechanical Behavior of Materials*, Stockholm (Edited by J. Carlsson and N. G. Ohlson). Pergamon Press, Oxford (1983).
7. J. W. Hutchinson, Constitutive behaviour and crack tip fields for materials undergoing creep-constrained grain boundary cavitation. *Acta Metall.* **31**, 1079 (1983).
8. V. Tvergaard, Constitutive relations for creep in polycrystals with grain boundary cavitation. *Acta Metall.* **32**, 1977 (1984).
9. V. Tvergaard, Effect of grain boundary sliding on creep constrained diffusive cavitation. *J. Mech. Phys. Solids* **33**, 447 (1985).
10. V. Tvergaard, Analysis of creep crack growth by grain boundary cavitation. *Int. J. Fracture* **31**, 183 (1986).
11. H. Riedel and J. R. Rice, *Tensile Cracks in Creeping Solids*, ASTM STP 700, p. 112. American Society for Testing and Materials, Philadelphia (1980).
12. J. L. Bassani and F. A. McClintock, Creep relaxation of stress around a crack tip. *Int. J. Solids Structures* **17**, 479 (1981).
13. M. Y. He and J. W. Hutchinson, *Bounds for Fully Plastic Crack Problems for Infinite Bodies*, ASTM STP 803, Vol. 1, p. 277. American Society for Testing and Materials, Philadelphia (1984).
14. O. C. Zienkiewicz and I. C. Corneau, Visco-plasticity plasticity and creep in elastic solids—a unified numerical solution approach. *Int. J. Numer. Meth. Engrg* **8**, 821 (1974).
15. R. Ehlers and H. Riedel, A finite element analysis of creep deformation in a specimen containing a macroscopic crack. In *Advances in Fracture Research, Proceedings of the Fifth International Conference on Fracture*, Cannes, 1981 (Edited by D. Francois *et al.*), p. 691. Pergamon Press, Oxford (1980).

#### APPENDIX: FINITE ELEMENT METHOD

In this work an incremental finite element scheme has been used. The scheme is equivalent to the more common direct stiffness formulation. The only difference is that in the incremental formulation the increments of nodal displacements are treated as unknowns. The material nonlinearity is taken care of using the initial strain

approach[14]. In this approach the inelastic strains are converted into equivalent body forces. The resulting equilibrium equation in incremental form is

$$[K]\{\Delta U\} = \{\Delta F\}^e + \{\Delta F\}^i \quad (\text{A1})$$

where  $\Delta U$  denotes the increments in the nodal displacements,  $\{\Delta F\}^e$  the increment in the applied nodal forces and  $\{\Delta F\}^i$  the increment in the pseudo load due to increase in the non-elastic strain. With this approach a linear finite element problem is obtained for each time step. The stiffness matrix in this formulation is the elastic stiffness matrix and is the same for all time steps. The solution of eqn (A1) gives the nodal displacement increments. From this, the increments in strains and stresses are calculated. These incremental values are integrated using an explicit, one-step Euler method. An automatic time step control scheme is used to balance the stability of the algorithm and the economy of the simulation run. During any time step the increment in the non-elastic strain is limited to a fraction " $f$ " of the accumulated creep strain such that

$$\dot{\epsilon}^n \Delta t \leq f \dot{\epsilon}^c. \quad (\text{A2})$$

The time step size is determined by keeping  $f$  in the range

$$0.05 < f < 0.1. \quad (\text{A3})$$

Formula (A3) is used as a guideline and time step size is never more than doubled in two consecutive steps. Also, after a maximum of three jumps in the time steps the calculations are re-stabilized using three constant length time steps.

Eight noded quadrilateral elements are used in the computation. The crack tip elements are formed by collapsing three nodes into one along one side. This element models a strain singularity of  $r^{-1}$  provided that the three collapsed nodes are allowed to displace independently. After the elastic solution is obtained in the first time step, these collapsed nodes are released to model the  $r^{-(\alpha/(\alpha+1))}$  singularity of the near tip strain field. A reduced ( $2 \times 2$ ) integration scheme is used to avoid the problem of modelling incompressible deformation for long times or near the crack tip.

To evaluate the path integral  $C$ , circular paths around the crack tip are selected. To avoid the additional calculation of stress and strains along any arbitrary path, these paths are selected to pass through the Gauss point locations of the elements. Twenty such paths (two in each of the ten radial layers of elements) are selected. The  $C$  line integral is evaluated using two point Gaussian quadrature over each of the eight line segments of the paths.